

## SIMPLE ONE-POT HYDROTHERMAL SYNTHESIS AND PHOTOCATALYTIC ACTIVITY OF ZnS AND ZnS/KAOLINITE NANOCOMPOSITE

Kateřina MAMULOVÁ KUTLÁKOVÁ<sup>1</sup>, Jonáš TOKARSKÝ<sup>1,2</sup>

<sup>1</sup>Nanotechnology Centre, VSB - Technical University of Ostrava, Ostrava, Czech Republic, EU,  
[katerina.mamulova.kutlakova@vsb.cz](mailto:katerina.mamulova.kutlakova@vsb.cz), [jonas.tokarsky@vsb.cz](mailto:jonas.tokarsky@vsb.cz)

<sup>2</sup>IT4Innovations, VSB - Technical University of Ostrava, Ostrava, Czech Republic, EU,  
[jonas.tokarsky@vsb.cz](mailto:jonas.tokarsky@vsb.cz)

### Abstract

This study is focused on preparation of pristine zinc sulphide (ZnS) and zinc sulphide/kaolinite (ZnS/K) nanocomposite using one-pot hydrothermal synthesis under atmospheric pressure and without any surfactant. Together with finding a simple preparation method, the aim was to achieve a high photocatalytic activity, and also reduce the environmental risk of ZnS (in the case of ZnS/K). Pristine ZnS was synthesized from aqueous solutions of zinc chloride and sodium sulphide in various ratios. ZnS/K nanocomposite was prepared similarly by addition of kaolin KKAF into the mixture of zinc chloride and sodium sulfide solutions. Reaction mixtures were continuously stirred at 100°C for several hours, resulting white solids were separated by centrifugation, washed with distilled water, and dried at 105°C overnight. X-ray powder diffraction analysis revealed the presence of cubic modification sphalerite both in ZnS and ZnS/K samples. Amount of ZnS in ZnS/K (~32 wt.%) was determined by Rietveld method which also confirmed the sphalerite structure. Morphology of the samples was observed using scanning electron microscopy. In the case of ZnS/K, the ZnS nanoparticles anchored on the kaolinite surface were observed. Photocatalytic activity evaluated using discoloration of Acid Orange 7 (AO7) in a liquid phase was found very high for ZnS samples. After 1 h of UV irradiation, ~99 % of AO7 was degraded by ZnS. Photodegradation efficiency reached 96 % in the case of ZnS/K. Taking into account that only ~32 wt.% of ZnS is present in ZnS/K, the photocatalytic activity of the nanocomposite can be considered three times higher compared to pristine ZnS.

**Keywords:** ZnS, kaolinite, hydrothermal synthesis, photoactivity, nanocomposite

### 1. INTRODUCTION

Zinc sulfide (ZnS), a direct wide band gap semiconductor crystallizing either in cubic sphalerite structure ( $E_g = 3.3\text{-}3.7$  eV) or hexagonal wurtzite structure ( $E_g = 3.7\text{-}3.9$  eV) [1], has found its application in many practical applications. In addition to medical diagnostics, sensing, and optoelectronic devices [2], the ZnS plays an important role also in the field of photocatalysis, and ZnS quantum dots [3], nanoparticles [4], or microparticles [5] were reported as suitable for this purpose. ZnS can be prepared from a range of zinc and sulphur precursors (zinc acetate [3,6], zinc chloride [7], zinc nitrate [4,5], thioacetamide [3], sodium sulphide [4,5], etc.) via various preparation methods including sonochemical synthesis [3], melting the precursors in autoclave at 210°C for 24 h [4], hydrothermal synthesis in autoclave at 180°C for 12 h [5], or low-temperature solid-state chemical synthesis [7]. Surfactants for controlling the size and preventing an agglomeration of ZnS are quite often used [6,7]. Since the free nanoparticles can be hazardous [8], it is reasonable to prepare nanocomposites in which the mobility of nanoparticles is limited. Earlier studies have shown clay minerals as suitable matrices for anchoring the nanoparticles. Moreover, these nanocomposites exhibit higher photocatalytic activity compared to pure nanoparticles [6,9]. Nanocomposites of clay/ZnS type are not reported as commonly as clay-based nanocomposites containing TiO<sub>2</sub> or ZnO. Only few works on montmorillonite/ZnS can be found, e.g., Kozák et al. [6] who reported a two-step synthesis in which pure ZnS nanoparticles were prepared and then anchored to pure MMT by shaking both components in aqueous solution. The aim of this work is to test the preparation of ZnS nanoparticles and ZnS containing nanocomposite by a simplified one-

step method without surfactants, without temperature higher than 100°C, and without complicated instrumentation. With respect to our earlier experiments [9], a similar preparation process and the same clay mineral, i.e., kaolinite KKAF, have been used in this work. X-ray powder diffraction, Rietveld analysis, and scanning electron microscopy were used to characterize the prepared samples. Finally, photoactivity of pure ZnS nanoparticles and the kaolinite/ZnS nanocomposite was determined and compared.

## 2. MATERIALS AND METHODS

### 2.1. Preparation of the samples

Zinc chloride (ZnCl<sub>2</sub>; anhydrous; Lach-Ner) and sodium sulphide (Na<sub>2</sub>S; anhydrous, Fisher Scientific) were used as received. For the preparation of pure ZnS nanoparticles, aqueous solutions of precursors having various concentrations (**Table 1**) were mixed in a beaker and continuously stirred at constant temperature 100°C. The kaolinite/ZnS nanocomposite was prepared similarly by mixing aqueous solutions of precursors in presence of 0.5 g of kaolinite KKAF (LB MINERALS). Size fraction < 40 μm was used. The resulting precipitates were centrifuged, washed with distilled water and dried at 100°C overnight. While the samples of pure ZnS nanoparticles were consecutively numbered, the nanocomposite was denoted as K/ZnS (**Table 1**).

**Table 1** Reaction conditions for the synthesis of ZnS nanoparticles and K/ZnS nanocomposite

sample	c(ZnCl <sub>2</sub> ) (mol/dm <sup>3</sup> )	c(Na <sub>2</sub> S) (mol/dm <sup>3</sup> )	molar ratio	m <sub>kaolinite</sub> (g)	reaction time (h)
ZnS_1	1.00	1.00	1:1	-	5
ZnS_2	0.50	1.00	1:2	-	5
ZnS_3	0.25	1.00	1:4	-	5
K/ZnS	0.50	1.00	1:2	0.5	4

### 2.2. Characterization methods

X-ray powder diffraction (XRPD) patterns were recorded (range 5-80°2θ) in reflection mode in symmetrical Bragg-Brentano arrangement using Bruker D8 Advance diffractometer equipped with fast position sensitive detector VANTEC 1. Radiation Co<sub>Kα</sub> was used (λ = 0.1789 nm). Sizes of ZnS crystallites (L<sub>c</sub>) were calculated from ZnS(111) reflection according to Scherrer formula [10]:

$$L_c = \frac{K\lambda}{\beta \cos \theta} \quad (1)$$

where K is the dimensionless shape factor (0.9 was used), λ is the radiation wavelength (nm), β is the full width at half maximum of the most intensive ZnS reflection, i.e., the ZnS(111) reflection (°), and θ is the position of the ZnS(111) reflection (°). Lanthanum hexaboride (LaB<sub>6</sub>) was used as a standard. Rietveld analysis (RA) of XRPD data was performed in Diffrac.Suite Topas software. Conditions of the RA were set up according to the experimental setting of the diffractometer, i.e., slit width 0.6 mm, Soller slits angle 2.3°, Lorentz polarization factor 0° (no monochromator). Chebyshev fifth-order polynomial was used for modeling the background. Goodness of fit was evaluated using χ<sup>2</sup> parameter [11] calculated via the least-square refinement of model XRPD pattern according to the experimentally obtained XRPD pattern. Scanning electron microscope (SEM) Hitachi SU6600 equipped with secondary electron detector was used to observe the samples. Prior the analysis, each sample was sputtered with Au/Pd. Accelerating voltage 5.0 kV was used. Photocatalytic experiment was performed in liquid phase using Acid Orange 7 (AO7). For each sample, two suspensions containing AO7 aqueous solution (V = 5 ml, c = 6.259·10<sup>-4</sup> mol/dm<sup>3</sup>), 65 ml of demineralized water, and 50 mg of the sample were stirred in the dark for 1 h in order to obtain the adsorption equilibrium. One suspension was subsequently stirred under UV irradiation (λ = 254 nm) for 1 h, the second one was stored in the dark.

Photocatalytic activity (PA) was evaluated using CINTRA 303 UV-VIS spectrometer according to the following equation:

$$PA(\%) = \left( 1 - \left( \frac{A_i}{A_c} \right) \right) \cdot 100 \quad (2)$$

where  $A_i$  and  $A_c$  is the intensity of AO7 absorption maximum (480 nm) for irradiated and control suspension, respectively.

### 3. RESULTS AND DISCUSSION

#### 3.1. Phase composition of the samples

XRPD analysis showed that all three samples ZnS\_1, ZnS\_2, and ZnS\_3 contain the same ZnS phase (**Figure 1a**), however, two options - sphalerite (PDF no. 05-0566) and wurtzite 8H (PDF no. 39-1363) - offered by ICDD PDF 2 Release 2014 database were very similar. Therefore, the RA was involved and two different models were used. Starting from unit cell parameters  $a = b = c = 5.409 \text{ \AA}$ ,  $\alpha = \beta = \delta = 90^\circ$  (sphalerite [12]) and  $a = b = 3.829 \text{ \AA}$ ,  $c = 25.041 \text{ \AA}$ ,  $\alpha = \beta = 90^\circ$ ,  $\delta = 120^\circ$  (wurtzite 8H polytype [13]), the RA (performed on ZnS\_3 pattern) revealed that the ZnS is present as the face centered cubic phase sphalerite. The  $\chi^2$  values 1.54 and 3.74 for sphalerite and wurtzite 8H, respectively, were obtained (compare also **Figures 1b and 1c**). For ZnS\_1, ZnS\_2, ZnS\_3 samples, the  $L_c$  values (Eq. 1) were 3.89 nm, 7.70 nm, 7.81 nm, respectively. Consistency of the increase in  $L_c$  values and the increase in  $\text{Na}_2\text{S} : \text{ZnCl}_2$  ratios (**Table 1**) is evident.

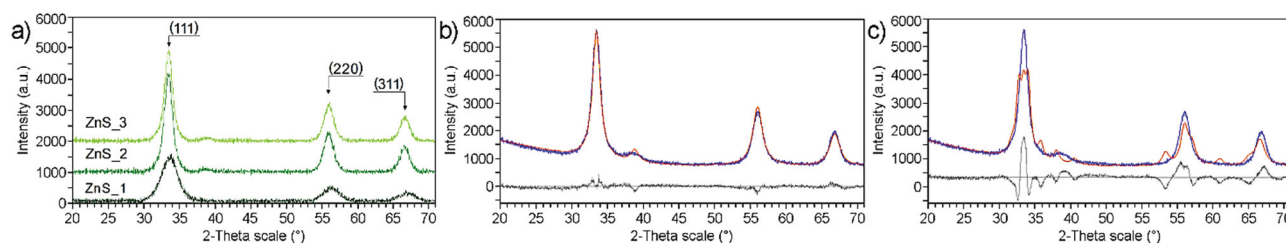


**Figure 1** (a) XRPD patterns of ZnS\_1, ZnS\_2, and ZnS\_3 sample in the range 20-70°2 $\theta$ . (b) Experimentally observed (ZnS\_3, blue), Rietveld calculated (red), and difference (grey bottom line) profiles for (b) sphalerite and (c) wurtzite 8H model applied to ZnS\_3 XRPD data

XRPD pattern of the K/ZnS nanocomposite (**Figure 2**) revealed four phases: kaolinite (PDF no. 58-2028), muscovite (PDF no. 58-2037), quartz (PDF no. 46-1045), and sphalerite (PDF no. 05-0566). The latter phase was confirmed again by the RA which was used also for quantitative determination of the K/ZnS composition (**Figure 2**). Starting from the cell parameters  $a = 5.155 \text{ \AA}$ ,  $b = 8.945 \text{ \AA}$ ,  $c = 7.405 \text{ \AA}$ ,  $\alpha = 91.70^\circ$ ,  $\beta = 104.86^\circ$ ,  $\delta = 89.82^\circ$  (kaolinite [14]),  $a = 5.189 \text{ \AA}$ ,  $b = 8.995 \text{ \AA}$ ,  $c = 20.097 \text{ \AA}$ ,  $\alpha = \delta = 90^\circ$ ,  $\beta = 95.11^\circ$  (muscovite [15]),  $a = b = 4.913 \text{ \AA}$ ,  $c = 5.405 \text{ \AA}$ ,  $\alpha = \beta = 90^\circ$ ,  $\delta = 120^\circ$  (quartz [16]), and the abovementioned cell parameters for sphalerite, the  $\chi^2$  value 2.26 for the XRPD pattern of K/ZnS sample was obtained. According to the quantitative RA, 49.16 wt.%, 11.85 wt.%, 7.26 wt.%, and 31.73 wt.% of kaolinite, muscovite, quartz, and sphalerite, respectively, is present in the K/ZnS nanocomposite. Good agreement between XRPD pattern and theoretical fit (**Figure 2**) indicates accuracy of the calculated weight percentages of individual phases in the K/ZnS sample. For ZnS in K/ZnS sample, value  $L_c = 4.83 \text{ nm}$  was obtained using Eq. (1). The size of crystallites is, therefore,  $\sim 1.6$  times lower compared to the ZnS\_2 sample which was prepared using the same  $\text{Na}_2\text{S} : \text{ZnCl}_2$  ratio as the K/ZnS (**Table 1**).

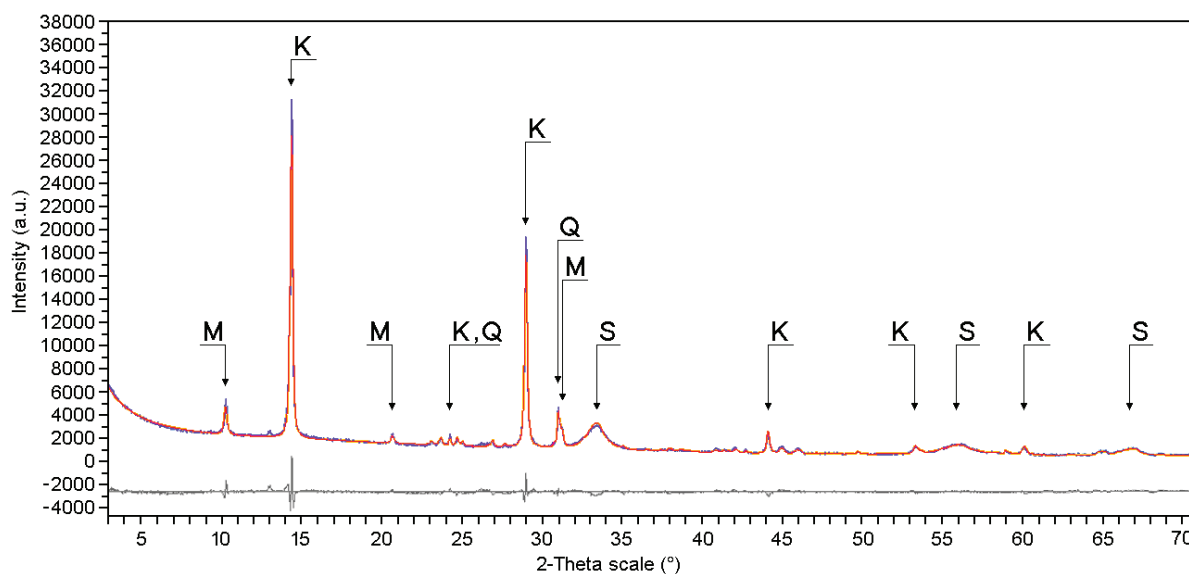


**Figure 2** Experimentally observed (blue), Rietveld calculated (red), and difference (grey bottom line) profiles for the K/ZnS nanocomposite. M - muscovite, K - kaolinite, Q - quartz, S - sphalerite.

### 3.2. Scanning electron microscopy

Morphology of pure ZnS (**Figures 3a-c**) and K/ZnS (**Figures 3d-f**), was studied using SEM analysis.

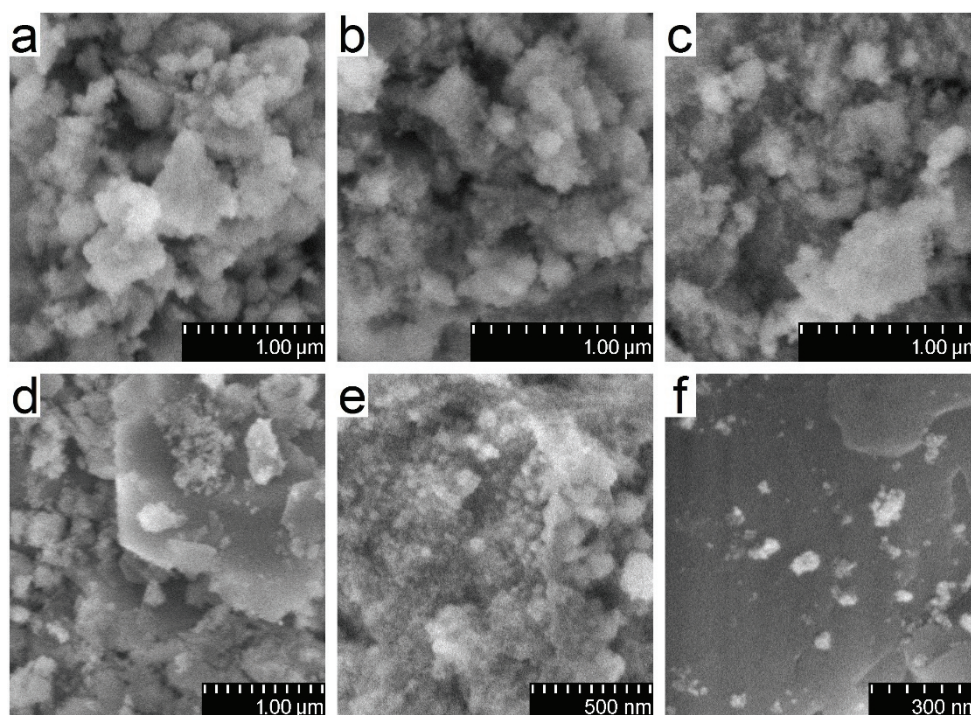


**Figure 3** SEM images of samples (a) ZnS\_1, (b) ZnS\_2, (c) ZnS\_3, and (d) K/ZnS

No significant differences between the pure ZnS samples were observed (**Figures 3a-c**), i.e., no influence of the  $\text{Na}_2\text{S} : \text{ZnCl}_2$  ratio on the morphology was found. A common feature is the high degree of agglomeration, however, although agglomerates reach sizes in the micrometer range, round shaped nanoparticles having size  $< 100$  nm can be recognized (**Figures 3a-c**). In the case of K/ZnS nanocomposite, SEM analysis confirmed the XRPD results in the meaning of ZnS growing on the clay matrix (**Figures 3d-f**). **Figure 3d** shows typical



hexagonally shaped particle of kaolinite covered by ZnS nanoparticles. Further observation of the K/ZnS nanocomposite revealed uneven coverage of the clay matrix by the ZnS nanoparticles. In addition to completely covered areas (**Figure 3e**), also the relatively empty areas with only few nanoparticles (more or less isolated) were found (**Figure 3f**). The nanoparticles observed on the surface at the greatest magnification (**Figure 3f**) have the size from units to tens of nanometers.

### 3.3. Photocatalytic activity

Photodegradation of AO7 revealed almost identical and very high PA values for all three samples ZnS\_1 (99.8 %), ZnS\_2 (100 %), and ZnS\_3 (99.2 %) (**Figure 4**). These results suggest negligible correlation between Na<sub>2</sub>S : ZnCl<sub>2</sub> ratio used and the resulting PA value. For K/ZnS nanocomposite, the PA value is slightly lower (95.6 %), however, significantly lower ZnS amount in this sample (31.73 wt.%; see section 3.1) compared to samples ZnS\_1, ZnS\_2, and ZnS\_3 (containing all 100 wt.% of ZnS) need to be kept in mind when evaluating the results. Thus, the ZnS in the K/ZnS nanocomposite exhibit nearly three times higher PA than pure ZnS nanoparticles when the ZnS amount in tested samples is taken into account. The observed increase in PA can be attributed to a lower degree of agglomeration of the ZnS nanoparticles in K/ZnS nanocomposite (see **Figures 3d,f**) due to their anchoring to the kaolinite matrix. The anchoring, along with a smaller size of nanoparticles, results in a higher area directly accessible to AO7 dye molecules.

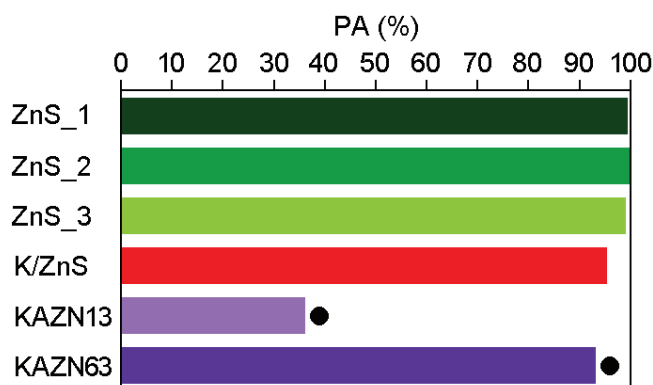


**Figure 4** Photocatalytic activity (PA) against AO7 after 1 h of UV irradiation. Calculated according to Eq. 2. Samples and PA values marked with • were taken from [9] for comparison.

The K/ZnS nanocomposite was also compared with kaolinite-based nanocomposite containing 30 wt.% of ZnO [9] (see KAZN13 in **Figure 4**). For the KAZN13 sample tested under the same conditions as in this work, PA = 36 % (**Figure 4**) was found [9], while to reach PA similar to the K/ZnS, the KAZN13 had to be calcined at 600 °C for 1 h (see KAZN63 in **Figure 4**) [9]. Unnecessity of the calcination step to obtain the same PA value is an important economic factor reducing the cost of K/ZnS preparation.

## 4. CONCLUSION

Pure ZnS nanoparticles and K/ZnS nanocomposite were successfully prepared using simple one-pot hydrothermal method under atmospheric pressure and without any surfactant. Qualitative XRPD analysis supported by RA confirmed sphalerite phase in prepared samples, quantitative analysis revealed 31.73 wt.% of the sphalerite in the K/ZnS nanocomposite. Morphology of the samples and anchoring of nanoparticles on the clay matrix was observed using SEM. For the pure ZnS samples, the photocatalytic experiment performed in liquid phase for 1 h under UV irradiation showed nearly complete degradation of AO7 dye. Slightly lower PA value 95.6 % was obtained for the K/ZnS sample, however, with respect to the ZnS amount (31.73 wt.%), the photoactivity of this nanocomposite can be considered very high. Unlike the previously prepared kaolinite-based nanocomposite containing 30 wt.% of ZnO, no calcination is needed in the case of K/ZnS to reach such

high PA value. The K/ZnS nanocomposite seems to be a very promising material for potential practical use in photocatalysis.

## ACKNOWLEDGEMENTS

***This work was supported by The Ministry of Education, Youth and Sports from the National Programme of Sustainability (NPS II) project „IT4Innovations excellence in science -LQ1602” and by the ERDF in the IT4Innovations national supercomputing center - path to exascale project (CZ.02.1.01/0.0/0.0/16\_013/0001791) within the OPRDE. Financial support from The Ministry of Education, Youth and Sports project no. SP2018/95 is also gratefully acknowledged. Authors thank Dalibor Hroch and Lukáš Herman for preparation of samples and Rietveld analysis.***

## REFERENCES

- [1] GAYOU, V. L., SALAZAR-HERNANDEZ, B. and CONSTANTINO, M.E. Structural studies of ZnS thin films grown on GaAs by RF magnetron sputtering. *Vacuum*. 2010. vol. 84, pp. 1191-1194.
- [2] UMMARTYOTIN, S. and INFHAUSAENG, Y. A comprehensive review on ZnS: From synthesis to an approach on solar cell. *Renewable and Sustainable Energy Reviews*. 2016. vol. 55, pp. 17-24.
- [3] GOHARSHADI, E. K., HADADIAN, M., KARIMI, M. and AZIZI-TOUPKANLOO, H. Photocatalytic degradation of reactive black 5 azo dye by zinc sulfide quantum dots prepared by a sonochemical method. *Materials Science in Semiconductor Processing*. 2013. vol. 16, no. 4, pp. 1109-1116.
- [4] XIANG, D., ZHU, Y., HE, Z., LIU, Z., and LUO, J. A simple one-step synthesis of ZnS nanoparticles via salt-alkali-composited-mediated method and investigation on their comparative photocatalytic activity. *Materials Research Bulletin*. 2013, vol. 48, no. 2, pp. 188-193.
- [5] ZHANG, S. Preparation of controlled-shape ZnS microcrystals and photocatalytic property. *Ceramics International*. 2014. vol. 40, no. 3, pp. 4553-4557.
- [6] KOZÁK, O., PRAUS, P., KOČÍ, K. and KLEMENTOVÁ, M. Preparation and characterization of ZnS nanoparticles deposited on montmorillonite. *Journal of Colloid and Interface Science*. 2010. vol. 352, no. 2, pp. 244-251.
- [7] CHEN, F., CAO, Y. and JIA, D. Facile synthesis of ZnS nanoparticles and their excellent photocatalytic performance. *Ceramics International*. 2015. vol. 41, pp. 6645-6652.
- [8] WU, T. and TANG, M. Review of the effects of manufactured nanoparticles on mammalian target organs. *Journal of Applied Toxicology*. 2018. vol. 38, no. 1, pp. 25-40.
- [9] MAMULOVÁ KUTLÁKOVÁ, K., TOKARSKÝ, J. and PEIKERTOVÁ, P. Functional and eco-friendly nanocomposite kaolinite/ZnO with high photocatalytic activity. *Applied Catalysis B: Environmental*. 2015. vol. 162, pp. 392-400.
- [10] SCHERRER, P. Estimation of size and internal structure of colloidal particles by means of Röntgen rays. *Nachrichten von der Gesellschaft der Wissenschaften zu Göttingen*. 1918. vol. 2, pp. 96-100.
- [11] TOBY, B. H. R factors in Rietveld analysis: How good is good enough? *Powder Diffraction*. 2006. vol. 21, no. 01, pp. 67-70.
- [12] WYCKOFF, R. W. G. *Crystal Structures, Volume 1*. 2<sup>nd</sup> ed. New York: John Wiley & Sons, p. 110.
- [13] CHAO, G. Y. and GAULT, R. A. The occurrence of two rare polytypes of wurtzite, 4H and 8H, at Mont Saint-Hilarie, Quebec. *The Canadian Mineralogist*. 1998. vol. 36, no. 3, pp. 175-177.
- [14] BISH, D. L. and VON DREELE, R. B. Rietveld refinement of non-hydrogen atomic positions in kaolinite. *Clays and Clay Minerals*. 1989. vol. 37, no. 4, pp. 289-296.
- [15] WYCKOFF, R. W. G. *Crystal Structures, Volume 4*. 2<sup>nd</sup> ed. New York: John Wiley & Sons, p. 346.
- [16] WYCKOFF, R. W. G. *Crystal Structures, Volume 1*. 2<sup>nd</sup> ed. New York: John Wiley & Sons, p. 312.